

Title No. 116-S41

Constitutive Model for Inelastic Buckling Behavior of Reinforcing Bars

by Yildir Akkaya, Serhan Guner, and Frank J. Vecchio

A refined constitutive model (called “RDM model”) is proposed for simulating the complete stress-strain response of longitudinal reinforcing bars, including the onset of inelastic buckling and subsequent degradation in the post-buckling regime. This model accounts for interactions between lateral ties and longitudinal bars, and is verified using 45 experimental and 58 analytical specimens previously tested by nine research groups. The RDM model is incorporated into a global modeling procedure and validated with six axially loaded columns, 16 axially and laterally loaded columns, and four beams previously tested by nine research groups. The validated procedure is used to study the influences of global second-order mechanisms such as geometrical nonlinearities, shear effects, and confinement effectiveness on the local buckling behavior. The proposed RDM model is shown to provide accurate response simulations for the buckling of reinforcing bars with a wide range of mechanical and geometrical properties. This model employs simple equations and defines full-range compressive response from well-known tensile material properties.

Keywords: inelastic buckling; nonlinear analysis; reinforced concrete elements; reinforcing bar; seismic performance; shear failure; steel reinforcement.

INTRODUCTION

The success of performance-based earthquake engineering (PBEE) hinges on accurately predicting the deformation response of structures under multiple seismic load levels. This requires computational simulation models that are capable of capturing significant post-peak behaviors at both global and local levels. The accuracy of the local response simulation is heavily influenced by the material models used in the definition of the stress-strain relations.

The longitudinal reinforcing bar response plays a crucial role in the seismic response of concrete buildings. Subjected to increasing compressive stresses, reinforcing bars undergo lateral displacements called “buckling” and exhibit significantly softened post-peak response, which signifies the end of the usable deformation capacity of a member. Many studies have examined the effects of buckling and provided experimental data, analytical data, and numerical models (refer to Table 1) offering invaluable insights into the buckling behavior of bare bars and isolated concrete elements.

Some studies proposed sophisticated constitutive models to simulate the buckling phenomenon; there are, however, challenges in incorporating these models into finite element analysis methods for the global modeling of buildings and bridges for PBEE. These challenges include: 1) compatibility issues between the buckling model formulations and the solution algorithm in the global analysis procedure; 2) limited applicability of each buckling model to reinforcing

bars with certain mechanical and geometrical properties; 3) the necessity of experimentally-determined special input parameters used in some buckling models; and 4) the prohibitive computational time required to perform buckling calculations for each finite element during each iteration. To address these challenges, a simple model with general applicability is required for engineers to accurately and effectively simulate the buckling behavior of reinforcing bars when performing the global analysis of structures.

RESEARCH OBJECTIVES

The objectives of this study are threefold: 1) establish a simple buckling model with a wide range of applicability; 2) incorporate it into a nonlinear global analysis procedure; and 3) study the influences of significant second-order mechanisms (for example, geometrical nonlinearity, shear effects, and confinement effectiveness) on the global response of concrete members, extending the present study beyond the influences tested experimentally in the literature. Other research goals include providing the engineering and research communities with the computer code of the established buckling model in an open-source format for incorporation into other computational simulation platforms (Akkaya et al. 2018), as well as the open-access version of the global analysis procedure VecTor5 (2018) with the proposed buckling model.

RESEARCH APPROACH

As the first step, a comprehensive literature review was conducted to categorize studies and computational models related to reinforcing bar buckling (refer to Table 1). In this process, the Dhakal and Maekawa model (2002a,b,c) (called “DM model” hereafter) was determined to be suitable for implementation into existing global analysis procedure VecTor5 (Guner and Vecchio 2010a,b) because: 1) it uses well-known tensile response parameters in defining the compressive response of reinforcing bars; 2) it has cyclic loading and unloading rules; 3) it has simple formulations that are compatible with the global analysis formulations to be employed; and 4) it was shown to provide accurate simulations of the post-buckling compression response of reinforcing bars. Dhakal and Maekawa (2002a) verified

ACI Structural Journal, V. 116, No. 3, March 2019.

MS No. S-2018-096, doi: 10.14359/51711143, was received March 17, 2018, and reviewed under Institute publication policies. Copyright © 2019, American Concrete Institute. All rights reserved, including the making of copies unless permission is obtained from the copyright proprietors. Pertinent discussion including author's closure, if any, will be published ten months from this journal's date if the discussion is received within four months of the paper's print publication.

Table 1—Previous studies on reinforcing bar buckling

Monotonic loading	Cyclic loading
Bae et al. 2005 ^{*,†,‡}	Cosenza and Prota 2006 [†]
Bayrak and Sheikh 2001 ^{†,‡,§}	Dhakar and Maekawa 2002c ^{*,§, ,#,††}
Berry and Eberhard 2005 ^{*,§}	Dodd and Restrepo-Posada 1995 [#]
Bresler and Gilbert 1961 [#]	Gomes and Appleton 1997 [*]
Gil-Martín et al. 2006 ^{*,}	Kim and Koutromanos 2016 [*]
Korentz 2010	Kunnath et al. 2009 ^{*,**}
Korentz and Marciniowski 2016	Mander et al. 1994 ^{†,***}
Mander et al. 1984 ^{†,§}	Monti and Nuti 1992 ^{†,†}
Mau and El-Mabsout 1989 ^{,§}	Nojavan et al. 2017 [†]
Massone and López 2014 ^{*,‡,††}	Pantazopoulou 1998 ^{§,#,††}
Massone and Moroder 2009 [‡]	Prota et al. 2009 [†]
Shanley 1947, 1950 [#]	Rodriguez et al. 1999 [†]
Urmson and Mander 2012 ^{*,#}	Su et al. 2015 ^{†,††}
Zong et al. 2013, 2014 ^{*,§}	Yang et al. 2016 [*]

*Buckling model.

†Experimental data.

‡Initial imperfection.

§Application.

||Analytical data.

#Theory.

**Low-cycle fatigue.

††Prediction for unsupported length.

the formulations of the DM model based on analytically generated data from 75 specimens using “COM3” (Concrete Model in 3D), a three-dimensional nonlinear finite element program (Tsuchiya et al. 1999; Maekawa et al. 2003).

Many more experimental and analytical buckling studies have been conducted since the introduction of the DM model in the literature; however, there have been no assessments of the accuracy and applicability of the DM model in simulating the response of these new specimens. As such, in this study the DM model was implemented into the computational procedure VecTor5 (2018) to model 45 experimental specimens tested by five research groups, as well as 58 analytical specimens tested by three research groups (refer to Fig. 1; refer to Tables A-1 and A-2 in the Appendix* for more details). At the conclusion of this process, the DM model was found to provide accurate response simulations without significantly increasing overall computational time or causing numerical problems. However, it was noted that the accuracy of the DM model diminishes for specimens with certain material properties and bar configurations, as will be discussed later.

To increase the applicability and accuracy of the DM model, three formulation refinements were made to create

*The Appendix is available at www.concrete.org/publications in PDF format, appended to the online version of the published paper. It is also available in hard copy from ACI headquarters for a fee equal to the cost of reproduction plus handling at the time of the request.

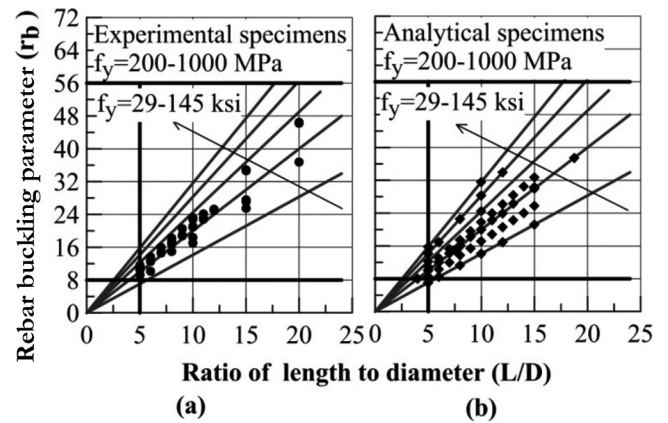


Fig. 1—Experimental and analytical database used in this study.

the Refined Dhakar-Maekawa (RDM) model. The refined formulations were verified by modeling 103 reinforcing bar specimens available in the literature. In the final part of this study, the RDM model was implemented into the global simulation procedure VecTor5 (2018) to model 26 large-scale reinforced concrete specimens, which validated the entire procedure and enabled analysis of the influences of global second-order effects on the local buckling response of longitudinal bars. This paper presents details of the refined formulation and verification studies, discusses the simulation accuracy improvements, and examines the critical parameters and limits that govern the inelastic buckling mechanism of reinforcing bars.

RESEARCH SIGNIFICANCE

Reinforcement buckling has been observed in structures damaged from recent earthquakes—even in buildings and bridges designed according to modern standards. Thus, it is important that numerical simulation methods are developed to account for this phenomenon and accurately determine the usable deformation capacities. Most existing buckling models are developed for a certain range of mechanical and geometrical properties, which limits their general applicability. In addition, most models are only available as research papers with no implementation into nonlinear analysis software. As such, this study aims to contribute to: 1) the creation of a simple and accurate buckling model with general applicability; 2) its incorporation into a global analysis procedure; and 3) the development of an open-source computer subroutine for the use of the community.

FORMULATION OF INELASTIC BUCKLING MODEL

The refined formulations of the RDM model are presented in Table 2 as compared with the original DM model. Definitions of variables are provided in the list of notations. In both models, the non-dimensional reinforcing bar buckling parameter r_b is calculated from Eq. (1) as a function of the square root of the yield stress (f_y), as well as the unsupported length-to-diameter ratio (L/D , shown in Fig. 2(a)) obtained using the procedure contained in Dhakar and Maekawa (2002c). The average compressive stress-strain response is derived from r_b and the tensile stress-strain response. When

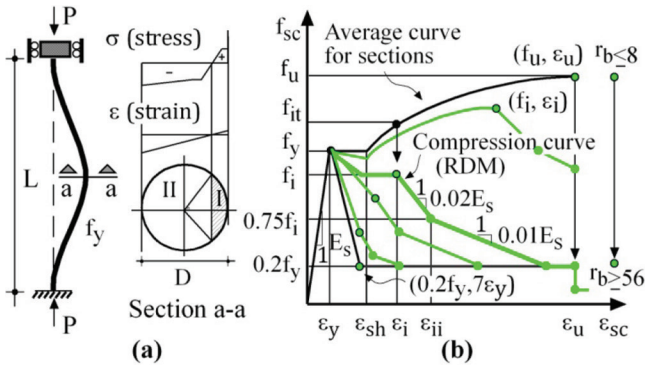


Fig. 2—Compressive stress-strain response of reinforcing bar as function of parameter r_b .

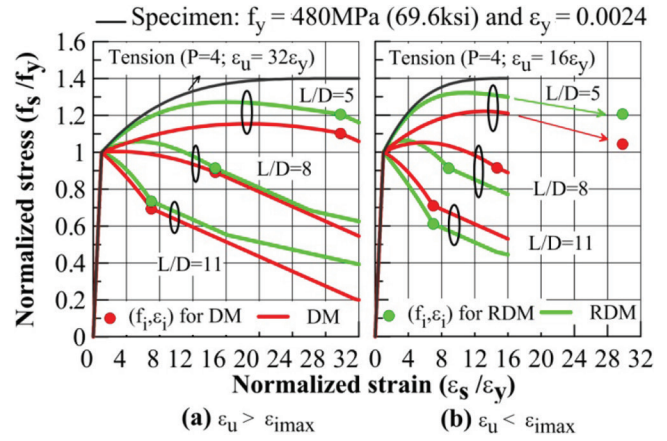


Fig. 3—Reinforcing bars with small ultimate strains.

Table 2—Comparison between formulations of DM and RDM models

DM model	RDM model
Input: $f_y, f_u, \epsilon_y, \epsilon_{sh}, \epsilon_u$, and L/D	
$P = 0, 1, \text{ and } 2$ (Selected)	$P = 0, 1, \text{ and } 4$ (Selected)
$r_b = (L/D)\sqrt{(f_y/100)}$ (f_y in MPa) and $\epsilon_i^0 = \epsilon_y(55 - 2.3r_b)$	
$r_{bmin} = 8$	$r_{bmin} = 5\sqrt{(f_y/100)}$ (f_y in MPa) for $(L/D)_{min} = 5$
$\epsilon_i = \epsilon_i^0$ and $\epsilon_i \geq 7\epsilon_y$	$\epsilon_i = \epsilon_i^0 \epsilon_u / \epsilon_{imax}$ for $\epsilon_i^0 < \epsilon_u < \epsilon_{imax}$; $\epsilon_i = \epsilon_i^0$ otherwise $\epsilon_{imax} = \epsilon_y(55 - 2.3r_{bmin})$ and $\epsilon_i \geq 7\epsilon_y$
$f_s = f_y$ for $\epsilon_s \leq \epsilon_{sh}$; $f_s = f_u$ for $\epsilon_s \geq \epsilon_u$; $f_s = f_u + (f_y - f_u)[(\epsilon_u - \epsilon_s)/(\epsilon_u - \epsilon_{sh})]^P$ for $\epsilon_{sh} < \epsilon_s < \epsilon_u$ where If $\epsilon_s = \epsilon_i \rightarrow f_s = f_{it}$; If $\epsilon_s = \epsilon_{sc} \rightarrow f_s = f_{st}$	
$f_i = f_i^0 = \alpha_1^0 \alpha_2 f_u^0$ $\alpha_1^0 = 0.75 + (\epsilon_u - \epsilon_{sh}) / (300\epsilon_y)$ $\alpha_1^0 \leq f_u / (1.5 f_y)$; $0.75 \leq \alpha_1^0 \leq 1.0$	$f_i = \alpha f_y$; $\alpha_1 = 0.8 + 1.8(f_u/f_y)(D/L)$ $\alpha = \alpha_1 \alpha_2$ for $\epsilon_i > \epsilon_{sh}$; $\alpha = 0.75 \alpha_1 \alpha_2$ for $\epsilon_i \leq \epsilon_{sh}$ $\alpha = 0.75 \alpha_2 (f_u/f_y)$ for $(\epsilon_u \leq \epsilon_{imax} \text{ and } \epsilon_i = 7\epsilon_y)$
$\alpha_2 = (1.1 - 0.016r_b)$ and $f_{it} \geq f_i \geq 0.2f_y$	
$f_{sc} = E_s \epsilon_{sc}$ for $\epsilon_{sc} \leq \epsilon_y$; $f_{sc} = f_{st} \{1 - (1 - f_i/f_{it})(\epsilon_{sc} - \epsilon_y)/(\epsilon_i - \epsilon_y)\}$ for $\epsilon_y < \epsilon_{sc} \leq \epsilon_i$	
$f_{sc} = f_i - 0.02E_s(\epsilon_{sc} - \epsilon_i)$ for $\epsilon_i < \epsilon_{sc} \leq \epsilon_u$	$f_{sc} = f_i - 0.02E_s(\epsilon_{sc} - \epsilon_i)$ for $\epsilon_i < \epsilon_{sc} \leq \epsilon_{ii}$; $\epsilon_{ii} = \epsilon_i + 0.25f_i/(0.02E_s)$ $f_{sc} = 0.75f_i - 0.01E_s(\epsilon_{sc} - \epsilon_{ii})$ for $\epsilon_{ii} < \epsilon_{sc} \leq \epsilon_u$
Output: $f_{sc} \geq 0.2f_y$	

defining the strain-hardening region of the tensile response from the yield point (f_y, ϵ_{sh}) up to the ultimate point (f_u, ϵ_u), the strain-hardening parameter P is taken as 4 in the RDM model as opposed to 2 in the DM model, as will be discussed later.

It is assumed that a reinforcing bar begins to buckle when the unsupported L/D is greater than or equal to 5 ($L/D \geq 5$). The minimum reinforcing bar buckling parameter r_{bmin} is calculated from Eq. (2) for the minimum L/D in the RDM model, as opposed to a constant value of 8 used in the DM model. The refined r_{bmin} calculation provides advantages when analyzing reinforcing bars with high yield strengths and small tie spacings, which are becoming more common in practice. For the maximum value of the reinforcing bar buckling parameter ($r_{bmax} \approx 56$ and $L/D \approx 28$ for $f_y = 400$ MPa [58 ksi]), both models consider the residual post-buckling compressive strain at an intermediate point of ($f_i = 0.2f_y, \epsilon_i = 7\epsilon_y$) as shown in Fig. 2(b).

The RDM model introduces three sets of formulation refinements. The first set is proposed with the aim of improving the simulation accuracy for bars with small ultimate strain values ($\epsilon_u < \epsilon_{imax}$) and small slenderness ratios ($r_b < 21$). For this case, using the original DM formulations, one can calculate the maximum intermediate strain $\epsilon_{imax} = \epsilon_i^0$ from Eq. (1) for $r_{bmin} = 8$. However, if $\epsilon_u < \epsilon_{imax}$, the average stress-strain point cannot reach the maximum intermediate point, which creates a theoretical gap (shown in Fig. 3(a) and (b)). To bridge this gap, the RDM model uses refined Eq. (3), where the $\epsilon_{imax} \geq \epsilon_i \geq 7\epsilon_y$ condition is always satisfied, along with a new definition of the minimum buckling parameter r_{bmin} in Eq. (2). This study also considered the analysis results of the specimens tested by Monti and Nuti (1992), which will be discussed later to show the improvements in simulation accuracy obtained with this refinement.

The second set of proposed refinements improves the simulation accuracy for reinforcing bars with a high hard-

ening parameter ($P = 4$) and relatively small values for the buckling parameter ($r_b < 21$). Many commonly used bars fall into this category; thus, this refinement has significant practical importance. Consider the determination of the intermediate stress (f_i^0) using the original DM formulations of Eq. (4), (5), and (6): f_i^0 is the stress on the tension curve corresponding to the intermediate strain (ϵ_i), and α_1^0 and α_2 are coefficients. α_2 was originally derived from an analytical parametric study by Dhakal and Maekawa (2002a). Coefficient α_1^0 was proposed by Dhakal and Maekawa (2002b) to account for the effects of material nonlinearity for $P=2$ ($0.75 \leq \alpha_1^0 \leq 1$). While modeling the specimens tested by Bayrak and Sheikh (2001) and Bae et al. (2005) (which had $P = 4$ and $r_b < 21$), it was noted that the DM formulations exhibit reduced prediction accuracy in the calculated responses. Kunnath et al. (2009) and Urmson and Mander (2012) also reported similarly reduced accuracy for such bars.

To overcome this issue while more effectively capturing the intermediate stress-strain point (f_i, ϵ_i), the RDM model proposes refined Eq. (5) and (6) based on an analytical study including all 103 specimens examined in this study. The refined formulations introduce a new coefficient α based on the location of the intermediate strain (ϵ_i) on the tension curve, as per Eq. (5). In the definition of α , a new coefficient α_1 is proposed to account for material nonlinearities. The last line of Eq. (5) includes a special case for $\epsilon_u \leq \epsilon_{imax}$ and $\epsilon_i = 7\epsilon_y$, for which the original DM formulation with the hardening parameter P of 1 is used. In the other two cases, a hardening parameter of 4 is used, which represents a more generalized formulation considering a wider variety of mechanical bar properties. As such, the RDM formulation does not use the ϵ_u, f_{it} , and P parameters for the calculation of the intermediate stress f_i (Eq. (5)) except for the special case of $\epsilon_u \leq \epsilon_{imax}$ and $\epsilon_i = 7\epsilon_y$. Consequently, the RDM model calculates the average compressive stress-strain (f_{sc}, ϵ_{sc}) response, as per Eq. (7) and (8). The analysis results of the specimens tested by Bayrak and Sheikh (2001) and Bae et al. (2005) will be discussed later to show the simulation accuracy improvements obtained with these refinements.

The third set of proposed refinements improves the general calculation accuracy when considering the entire dataset of 103 specimens. The original DM formulation uses a linear descending branch with a constant negative slope of 2% of E_s after the intermediate stress-strain point (f_i, ϵ_i). Comparisons with the entire experimental database and the model proposed by Bae et al. (2005) shows that bilinear response provides more accurate response simulations. As such, the RMD model proposes bilinear negative post-buckling stiffnesses, as per Eq. (8).

VERIFICATION WITH REINFORCING BAR SPECIMENS

Experimental specimens

The experiment dataset found in the literature consists of 45 reinforcing bar specimens—three specimens tested by Mander et al. (1984), five by Monti and Nuti (1992), six by Bayrak and Sheikh (2001), 16 by Bae et al. (2005), and 15 by Prota et al. (2009). These specimens incorporate the following ranges: unsupported length ratios of $5 \leq L/D$

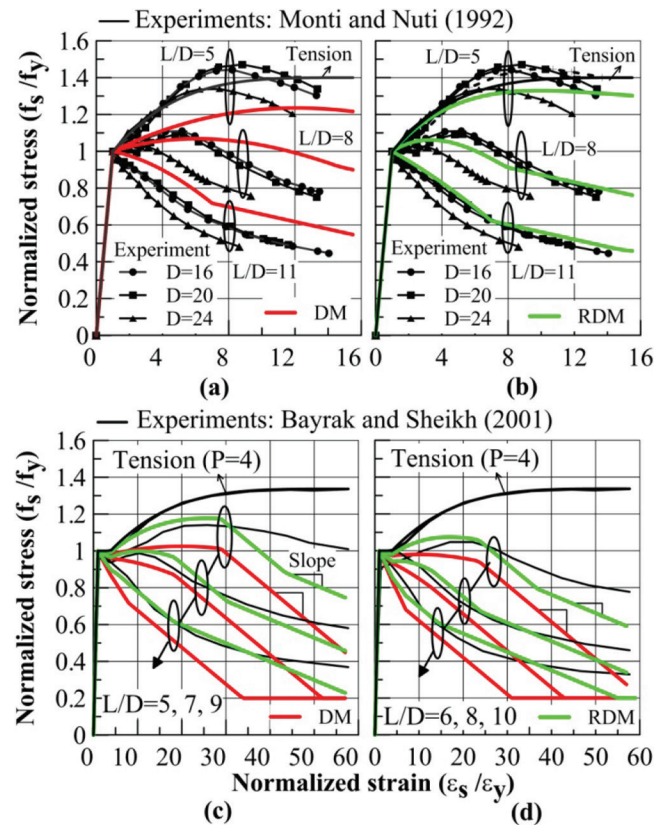


Fig. 4—Verification with experimental data.

≤ 20 ; yield stresses of 295 MPa (42.8 ksi) $\leq f_y \leq 540$ MPa (78.3 ksi); and ultimate strength-to-yield strength ratios of $1.2 \leq f_u/f_y \leq 1.6$. Refer to Table A-1 for complete details of experiment dataset.

To evaluate the improvements achieved with the first set of refinements, consider Fig. 4(a) and (b), which includes three bar diameters of 16, 20, and 24 mm (0.63, 0.79, and 0.95 in.), as well as three L/D ratios of 5, 8, and 11. While the ultimate strain ϵ_u was approximately $16\epsilon_y$, the maximum intermediate strain ϵ_{imax} was $30\epsilon_y$ for the specimens with $L/D = 5$. For these specimens, when using the DM model formulations, the ultimate stress-strain point is reached before reaching the intermediate point; this phenomenon results in premature failures due to material nonlinearity, not reinforcing bar buckling (refer to Fig. 4(a)). As seen in Fig. 4(b), the revised formulations rectify this anomaly and improve the simulation accuracy for reinforcing bars with small ultimate strains in tension (for example, $\epsilon_u < \epsilon_{imax}$ where $\epsilon_{imax} = 39\epsilon_y$ for $f_y = 200$ MPa [29 ksi] and $\epsilon_{imax} = 20\epsilon_y$ for $f_y = 900$ MPa [130 ksi]).

To demonstrate the improvements achieved by the second and third sets of refinements, consider Fig. 4(c) and (d). The specimens contained in both experimental sets had tensile stress-strain curves with a highly nonlinear hardening response (that is, $P = 4$). As shown in Fig. 4(c), the DM model could not accurately capture the intermediate stress-strain points for the different unsupported length ratios (L/D). In addition, the experimentally obtained negative slopes were not constant after the intermediate point, unlike the assumption made in the DM model. The RDM model more accurately calculates the intermediate point and

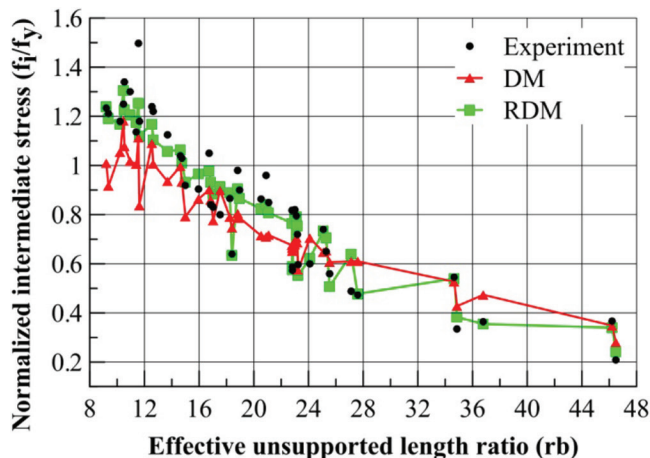


Fig. 5—Comparisons of calculated intermediate points with experimental data.

the post-buckling negative stiffnesses, as shown in Fig. 4(c) and (d). The improvement in the prediction accuracy is more significant for specimens with small unsupported length ratios (that is, $L/D = 5$ and 6). Refer to Fig. A-1(a) for validation with another experiment-based dataset.

Figure 5 compares the responses obtained from the DM and RDM models in terms of the normalized intermediate stress (f_i/f_y) for the entire experiment dataset of 45 specimens. The normalized intermediate stresses (that is, α in Eq. (5)) for each specimen are calculated from the formulations of the DM and RDM models. In addition, the normalized experimental stresses are extracted from the experimental average compressive stress-strain curves of the specimens for the same intermediate strain (ϵ_i) and the same reinforcing bar buckling parameter (r_b). Figure 5 demonstrates that the RDM model provides more accurate response simulations, especially for specimens with buckling parameters smaller than 21.

Analytical specimens

To verify that the refinements do not result in any reduced accuracy, the original analytical database used in the development of the DM model was analyzed using the RDM model. Figure 6 presents the analysis results for the specimens with a yield stress of 400 MPa (58 ksi) and two different response characteristics, including elastic-plastic and elastic-plastic-linear hardening responses in tension; refer to Fig. A-1(b) for the analysis results of the other specimens with a yield stress of 800 MPa (116 ksi). It is clear that the results obtained from the RDM model provides a similar accuracy to those obtained from the DM model. In addition, the results of the RDM model are independent of the value of the hardening parameter P .

To further test the RDM model, a new dataset with 41 additional analytical specimens was modeled, using the data produced by Mau and El-Mabsout (1989), Gil-Martín et al. (2006), and Korentz (2010). Table A-2 provides the mechanical properties of the specimens. The tension responses of the analytical specimens were defined to be the same up to the maximum intermediate strain (ϵ_{imax}) level while applying the formulations of both models to these analytical spec-

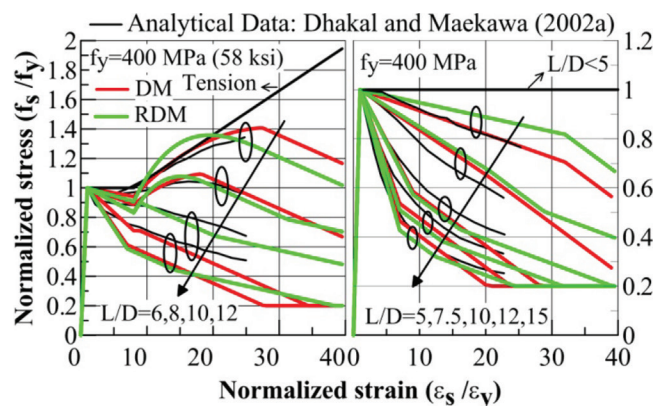


Fig. 6—Verification with original analytical data.

imens. Figure A-2 shows the simulation results obtained from these specimens. It was observed that the difference between the results is only a function of the reinforcing bar buckling parameter (r_b) or L/D in the applications of DM and RDM models, supporting the findings of Dhakal and Maekawa (2002a). Therefore, it can be stated that the inelastic buckling mechanism and the ductility capacity of reinforcing bars are mainly controlled by r_b and support conditions, while material nonlinearity has a relatively small effect. Additionally, Fig. A-3 compares the normalized intermediate stress (f_i/f_y) values obtained from both models to show the differences in the region of $r_b < 21$.

VERIFICATION WITH REINFORCED CONCRETE SPECIMENS

Global modeling process

To further verify the established formulations, as well as study the influence of the global mechanisms on the local buckling response, both the DM and RDM reinforcing bar buckling models were implemented into the global modeling procedure VecTor5 (Guner and Vecchio 2008, 2010a,b), which is a specialized nonlinear analysis method for two-dimensional RC frame structures. VecTor5 employs six-degree-of-freedom, distributed-plasticity elements (as shown in Fig. 7(a)) and uses an iterative, total-load, secant-stiffness formulation. The nonlinear sectional analysis algorithms can model the concrete response, including the shear effects coupled with axial and flexural responses, based on the Disturbed Stress Field Model (DSFM) (Vecchio 2000).

The DSFM accounts for local crack conditions as well as yielding and strain hardening of the reinforcement at a crack. A fiber discretization of the cross-section is employed, as illustrated in Fig. 7(b). Each concrete and longitudinal reinforcing bar layer is defined as a discrete element. The triaxial concrete core confinement is accounted for through in- and out-of-plane reinforcement components; refer to Fig. 7(c) for a sample response. The main sectional compatibility requirement is that “plane sections remain plane,” while the sectional equilibrium requirements include balancing the axial force, shear force, and bending moment. To compensate for the clamping stresses in the transverse direction (assumed to be zero) and prevent premature failures of D-regions, a shear protection algorithm is employed. In addition, the procedure incorporates several second-order

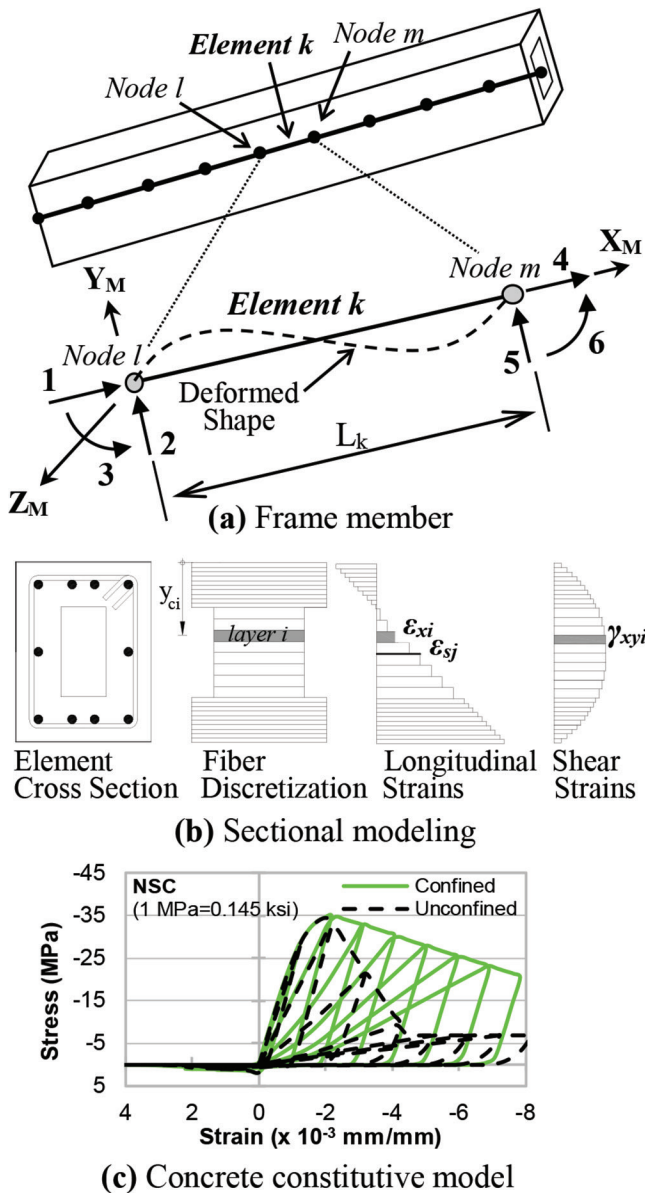


Fig. 7—Global modeling procedure.

material behaviors that are specific to reinforced concrete structures, as listed in Table A-3.

The numerical models were created using the published specimen details, with the help of a pre-processor program FormWorks-Plus (Sadeghian 2012; Blosser et al. 2016). The default models used for the material modeling throughout this study are listed in Table A-3. The results studied included the load-deflection responses, member deformations, concrete crack locations propagation and widths, reinforcement stresses and strains, and the failure modes and displacements. The analysis results were visually studied through the graphical post-processor program Janus (Chak 2013; Loya et al. 2016).

Axially loaded columns

An experiment dataset including six large-scale columns (LS1, LS4, and LW1 through LW4), tested by Hoshikuma et al. (1997), were examined to verify the RDM model as implemented into the global analysis program VecTor5

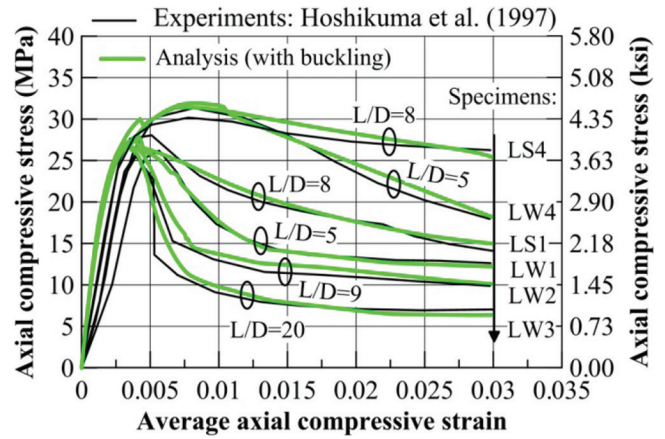


Fig. 8—Axially loaded column specimens.

(2018), and to study the influence of the confinement effectiveness of the lateral ties after the initiation of bar buckling. All columns had L/D ratios greater than 5, and thus exhibited reinforcement buckling in the experimental tests. The sectional details of the specimens are presented in Fig. A-4(a).

The numerical models were created using the reported material properties. The following values were assumed for any unreported longitudinal reinforcement properties: ultimate strength $f_u = 1.5f_y$, yield strain $\epsilon_y = 0.00164$, initial hardening strain $\epsilon_{sh} = 6\epsilon_y$, and ultimate strain $\epsilon_u = 110\epsilon_y$. Formulations by Mander et al. (1988) were used when defining the out-of-plane reinforcement ratio (ρ_z). As shown in Fig. 8, the analysis results captured the experimental behaviors well. Both DM and RDM models provided similar global response simulation results with limited reinforcing bar buckling due to the low longitudinal reinforcement ratios (that is, 1%) contained by these specimens. The analysis results indicate that the reinforcing bar buckling mechanism results in a decrease in the confinement effectiveness of the lateral ties by approximately $1/3\rho_z$. This decrease was determined using the confinement effectiveness factor k_e , a method proposed by Mander et al. (1988).

Axially and laterally loaded columns

An experiment dataset totaling 16 columns, tested by seven research groups—Tanaka and Park (1990), Bayrak and Sheikh (1997), Saatcioglu and Ozcebe (1989), Soesi-anawati et al. (1986), Xiao and Martirosyan (1998), Sezen and Moehe (2002), and Lynn et al. (1996)—were modeled to further test the RDM model and to study the influence of buckling on the confinement effectiveness on the core concrete.

Based on the test configurations, the columns are categorized into three geometrical groups, namely: the flexible-base (CFB), the double curvature (DC), and the double-ended (DE) models (as shown in Fig. 9), as well as two behavior modes, namely: flexure- and shear-critical. Refer to Tables A-4 to A-6 for complete geometrical and mechanical properties.

Figure 10 shows the analysis results for four columns exhibiting flexure-critical behavior; refer to Fig. A-5(a) for the remaining four specimens. Specimens S3 and U3 had

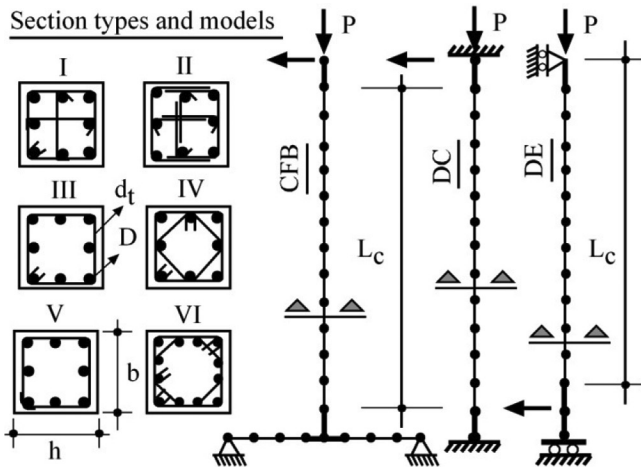


Fig. 9—Numerical models of axially and laterally loaded columns.

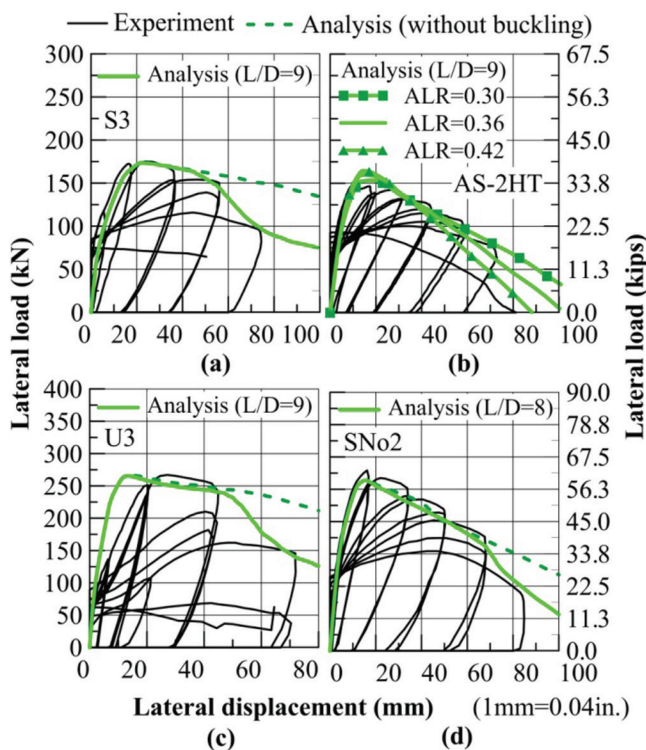


Fig. 10—Verification with columns in flexural failure.

sectional details that were particularly vulnerable to reinforcing bar buckling, despite being subjected to low levels of axial loads. Specimen S3 had open U-shaped stirrups (that is, DE-Type II in Fig. 9), while Specimen U3 had closed stirrups (that is, CFB-Type III) with a high longitudinal reinforcement ratio of 3.2% and a large bar diameter of 25 mm (1 in.). The global simulation procedure was able to capture the buckling phenomenon and associated post-buckling softening behavior for both specimens, as shown in Fig. 10(a) and (c). Examination of the analysis output revealed that the buckled bars resulted in a decrease of approximately $1/3\rho_z$ in the confinement effectiveness of lateral ties on the confined concrete core.

Specimens AS-2HT and SNo2 had DE-Type IV and DE-Type VI sections, respectively, with well-confined cores,

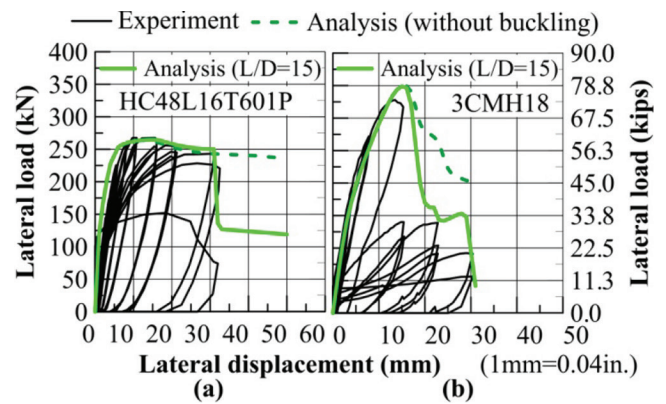


Fig. 11—Verification with columns in shear failure.

a longitudinal reinforcement ratio of 2.6% and 1.5%, and an axial load ratio of 0.36 and 0.30. In the experimental study, reinforcing bar buckling took place shortly after reaching a lateral displacement of 70 mm (2.8 in.) in both specimens (refer to Fig. 10(b) and (d)). The analyses successfully captured the buckling effects and demonstrated that high levels of axial loads coupled with bending effects dominated the responses of both columns. Moreover, the analysis results of Specimen AS-2HT in Fig. 10(b) demonstrate the influence of the axial load ratios (ALR) on the ductility capacity of the specimen.

Figure 11 shows the analysis results for two columns exhibiting shear-critical behavior; refer to Fig. A-4(b) and A-5(b) for the remaining six columns. In all columns, the longitudinal reinforcing bars had large slenderness ratios with L/D ratios ranging from 10 to 15, and thus exhibited significant reinforcement buckling in the experimental studies. The analyses successfully captured the buckling effects (refer to Fig. 11) and demonstrated that having an accurate reinforcing bar buckling model is not enough to capture the ductility capacities of these columns without considering the shear-critical behaviors.

Beams in bending

Four reinforced concrete beams (S1B2, S1B3, S3B2, and S3B3), tested by Lopes et al. (2012), were modeled. The test program included a four-point bending setup, where the compression bars were subjected to buckling in the middle regions with pure bending conditions. Refer to Fig. A-6(a) and Tables A-7 to A-9 for the complete details of the specimens. It should be noted that the tension reinforcement ratio used in these specimens (2.5%) was greater than the balanced reinforcement ratio.

Analysis results (with and without accounting for reinforcing bar buckling) are compared with the experimental results for each beam in Fig. 12, where the tension, transverse, and out-of-plane reinforcement ratios (ρ , ρ_t , and ρ_z) of each specimen are also shown. Refer to Fig. A-6(b) for the other two beams. The global analysis procedure captured the reinforcing bar buckling effects well. The most significant strength softening was observed in Specimen S1B3, where reinforcing bar buckling and confinement effects were high due to the reinforcement configurations. Parametric analyses performed showed that the confinement effectiveness of the

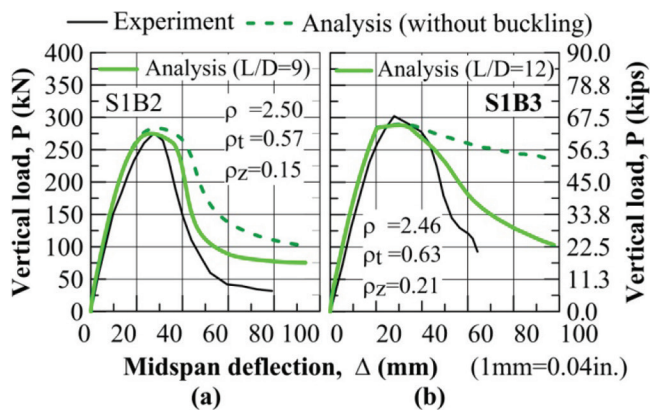


Fig. 12—Verification with beams tested by Lopes et al. (2012).

lateral ties on the confined concrete core is reduced up to two-thirds due to reinforcing bar buckling.

SUMMARY AND CONCLUSIONS

This paper presents a new constitutive model (RDM) for simulating the buckling response of compression bars in concrete members, based on the refinement of the Dhakal-Maekawa (DM) model. The material-level studies conducted in this study support the following conclusions:

1. The RDM model is shown to provide more accurate stress-strain response simulations, as compared to the DM model, for reinforcing bars experiencing lateral deformations (that is, buckling) with a wide range of mechanical and geometrical properties—for example, $200 \text{ MPa} (29 \text{ ksi}) < f_y < 900 \text{ MPa} (131 \text{ ksi})$, $10 \text{ mm} (0.4 \text{ in.}) < D < 36 \text{ mm} (1.4 \text{ in.})$, $f_u/f_y < 2$, $P \leq 4$, $\epsilon_u > 14\epsilon_{ys}$, $8 < r_b < 56$, and $L/D \geq 5$.

2. The RDM model provides modeling simplifications as compared to the DM model by not using the strain hardening parameter (P) and ultimate strain (ϵ_u) values in the determination of the intermediate stress-strain point, as well as by using a fixed strain hardening parameter in the remaining parts of the response.

3. The RDM model provides advantages for the cases where the ultimate strain ϵ_u on the tension curve is unknown or approximated, because the formulation of the RDM model is less sensitive to the ϵ_u value.

4. It is confirmed that the average compressive stress-strain curve can be obtained from a single non-dimensional parameter r_b (a function of the unsupported length-to-diameter ratio and the yield stress of the reinforcing bar) when the tension stress-strain curve, material properties, and support conditions are known.

The member-level global modeling studies conducted support the following conclusions:

1. Accurate simulation of the force-deflection, shear, and confined concrete behaviors are crucial pre-requisites for accurately capturing the reinforcing bar buckling mechanisms, which typically occur towards the end of the post-peak softening region of the global response.

2. The confinement effectiveness of stirrups on the confined concrete core was found to decrease by approximately one-third once reinforcing bar buckling takes place for flexure-controlled columns. For shear-controlled columns, both

shear and reinforcing bar buckling effects should be taken into account for accurate response simulations.

3. A simple, non-iterative buckling model is required to keep the computational demand within reasonable limits. In this study, the longest analyses required took approximately one minute of computational time, for both DM and RDM models, when obtaining the complete monotonic load-deformation response using a high-speed processor (3M cache, 2.40 GHz) and 3 GB RAM.

4. The direct stiffness method was found to be an effective platform for incorporating the geometric and material nonlinearity formulations, without a need for an implicit solution algorithm.

5. For compression-controlled sections subjected to bending, reinforcing bar buckling effects are found to influence the post-peak softening behavior significantly. For sections in the transition zone, buckling effects had some influence on the post-peak behavior. For tension-controlled sections, the effects of reinforcing bar buckling were found to be insignificant in most cases.

6. Further numerical and experimental studies should be undertaken to verify the simulation accuracy when modeling the influence of bar buckling on the holistic response of large-frame buildings subjected to seismic ground excitation.

AUTHOR BIOS

Yildir Akkaya is a Research Assistant in the Department of Civil Engineering, Faculty of Civil Engineering, at Istanbul Technical University, Istanbul, Turkey, where he received his PhD. His research interests include analysis, design, performance assessment, repairing, and strengthening of reinforced concrete structures for earthquake resistance; finite element modeling; and nonlinear analysis of reinforced concrete structures.

ACI member Serhan Guner is an Assistant Professor in the Department of Civil Engineering at the University of Toledo, Toledo, OH. He received his PhD from the University of Toronto, Toronto, ON, Canada. He is a member of Joint ACI-ASCE Committee 447, Finite Element Analysis of Reinforced Concrete Structures. His research interests include finite element modeling of concrete and wood structures, shear effects in concrete, structural response to extreme loads, and development of analysis tools for use in practice.

Frank J. Vecchio, FACI, is a Professor in the Department of Civil Engineering at the University of Toronto. He is a member of Joint ACI-ASCE Committees 441, Reinforced Concrete Columns, and 447, Finite Element Analysis of Reinforced Concrete Structures. He received the following ACI awards: Structural Research Award in 1998; Structural Engineering Award in 1999; Wason Medal for Most Meritorious Paper in 2011; and the Joe W. Kelley Award in 2016. His research interests include advanced constitutive modeling and analysis of reinforced concrete, assessment and rehabilitation of structures, and response to extreme loads.

ACKNOWLEDGMENTS

The writers gratefully acknowledge the Scientific and Technological Research Council of Turkey (TUBITAK), Science Fellowships and Grant Programs-in-aid for scientific research No. 2219 (BIDEB-2219) for providing financial support to accomplish this research.

NOTATION

D	=	diameter of longitudinal reinforcing bar
d_t	=	diameter of transverse reinforcing bar
f_i^0, ϵ_i^0	=	stress and strain at intermediate point in DM model
f_i, ϵ_i	=	stress and strain at intermediate point in RDM model
f_{it}^0, f_{it}	=	stresses corresponding to intermediate strain ϵ_i on tension stress-strain curve
f_{sc}, ϵ_{sc}	=	current compressive stress and strain of reinforcing bar including buckling
f_{st}	=	stress corresponding to current strain ϵ_{sc} on tension stress-strain curve

f_u, ϵ_u	=	ultimate strength and strain on tension stress-strain curve
L	=	unsupported length of longitudinal reinforcing bar
L_c	=	length of column specimen
r_b	=	non-dimensional reinforcing bar buckling parameter
r_{bmin}	=	minimum value of reinforcing bar buckling parameter, calculated from $(L/D = 5)$
s	=	spacing of transverse reinforcing bars or stirrups
α	=	intermediate stress to yield stress ratio (f_i/f_y)
α_1^0	=	coefficient to determine f_i^0 in DM model
α_1	=	coefficient to determine f_i in RDM model
α_2	=	coefficient used in both DM and RDM models
ϵ_{ii}	=	strain corresponding to stress of $0.75f_i$ in RDM model
ϵ_{imax}	=	maximum strain at intermediate point and calculated from r_{bmin}
ϵ_{sh}	=	initial hardening strain on tension stress-strain curve
ρ	=	longitudinal reinforcement ratio
ρ_t	=	transverse reinforcement ratio
ρ_z	=	out-of-plane reinforcement ratio

REFERENCES

- Akkaya, Y.; Guner, S.; and Vecchio, F. J., 2018, "RDM Model for the Inelastic Buckling Behavior of Reinforcing Bars," <http://www.utoledo.edu/engineering/faculty/serhan-guner/Software.html>. (last accessed Jan. 7, 2019)
- Bae, S.; Mises, M. A.; and Bayrak, O., 2005, "Inelastic Buckling of Reinforcing Bars," *Journal of Structural Engineering*, ASCE, V. 131, No. 2, pp. 314-321. doi: 10.1061/(ASCE)0733-9445(2005)131:2(314)
- Bayrak, O., and Sheikh, S. A., 1997, "High Strength Concrete Columns under Simulated Earthquake Loading," *ACI Structural Journal*, V. 94, No. 6, Nov.-Dec., pp. 708-722.
- Bayrak, O., and Sheikh, S. A., 2001, "Plastic Hinge Analysis," *Journal of Structural Engineering*, ASCE, V. 127, No. 9, pp. 1092-1100. doi: 10.1061/(ASCE)0733-9445(2001)127:9(1092)
- Berry, M. P., and Eberhard, M. O., 2005, "Practical Performance Model for Bar Buckling," *Journal of Structural Engineering*, ASCE, V. 131, No. 7, pp. 1060-1070. doi: 10.1061/(ASCE)0733-9445(2005)131:7(1060)
- Blosser, K.; Guner, S.; and Vecchio, F. J., 2016, "User's Manual of FormWorks Plus for VecTor5," Department of Civil Engineering, University of Toledo, Toledo, OH, 29 pp., http://www.utoledo.edu/engineering/faculty/serhan-guner/docs/M3_VT5FWPManual.pdf. (last accessed Jan. 7, 2019)
- Bresler, B., and Gilbert, P. H., 1961, "Tie Requirements for Reinforced Concrete Columns," *ACI Journal Proceedings*, V. 58, No. 5, May, pp. 555-570.
- Chak, I., 2013, "Janus: A Post-Processor for VecTor Analysis Software," MASC thesis, Department of Civil Engineering, University of Toronto, Toronto, ON, Canada, 193 pp.
- Cosenza, E., and Prota, A., 2006, "Experimental Behavior and Numerical Modeling of Smooth Steel Bars under Compression," *Journal of Earthquake Engineering*, V. 10, No. 3, pp. 313-329. doi: 10.1080/13632460609350599
- Dhakar, R. P., and Maekawa, K., 2002a, "Modeling for Postyield Buckling of Reinforcement," *Journal of Structural Engineering*, ASCE, V. 128, No. 9, pp. 1139-1147. doi: 10.1061/(ASCE)0733-9445(2002)128:9(1139)
- Dhakar, R. P., and Maekawa, K., 2002b, "Path-Dependent Cyclic Stress-Strain Relationship of Reinforcing Bar Including Buckling," *Engineering Structures*, V. 24, No. 11, pp. 1383-1396. doi: 10.1016/S0141-0296(02)00080-9
- Dhakar, R. P., and Maekawa, K., 2002c, "Reinforcement Stability and Fracture of Cover Concrete in Reinforced Concrete Members," *Journal of Structural Engineering*, ASCE, V. 128, No. 10, pp. 1253-1262. doi: 10.1061/(ASCE)0733-9445(2002)128:10(1253)
- Dodd, L. L., and Restrepo-Posada, J. I., 1995, "Model for Predicting Cyclic Behavior of Reinforcing Steel," *Journal of Structural Engineering*, ASCE, V. 121, No. 3, pp. 433-445. doi: 10.1061/(ASCE)0733-9445(1995)121:3(433)
- Gil-Martín, L. M.; Hernández-Montes, E.; Aschheim, M.; and Pantazopoulou, S. J., 2006, "Slenderness Effects on the Simulated Response of Longitudinal Reinforcement in Monotonic Compression," *Structural Engineering and Mechanics*, V. 23, No. 4, pp. 369-386. doi: 10.12989/sem.2006.23.4.369
- Gomes, A., and Appleton, J., 1997, "Nonlinear Cyclic Stress-Strain Relationship of Reinforcing Bars Including Buckling," *Engineering Structures*, V. 19, No. 10, pp. 822-826. doi: 10.1016/S0141-0296(97)00166-1
- Guner, S., and Vecchio, F. J., 2008, "User's Manual of VecTor5," Online Publication, 88 pp., www.utoledo.edu/engineering/faculty/serhan-guner/docs/M1-VT5Manual-V1.2.pdf. (last accessed Jan. 7, 2019)
- Guner, S., and Vecchio, F. J., 2010a, "Pushover Analysis of Shear-Critical Frames: Formulation," *ACI Structural Journal*, V. 107, No. 1, Jan.-Feb., pp. 63-71.
- Guner, S., and Vecchio, F. J., 2010b, "Pushover Analysis of Shear-Critical Frames: Verification and Application," *ACI Structural Journal*, V. 107, No. 1, Jan.-Feb., pp. 72-81.
- Hoshikuma, J.; Kawashima, K.; Nagaya, K.; and Taylor, A. W., 1997, "Stress-Strain Model for Confined Reinforced Concrete in Bridge Piers," *Journal of Structural Engineering*, ASCE, V. 123, No. 5, pp. 624-633. doi: 10.1061/(ASCE)0733-9445(1997)123:5(624)
- Kim, S. H., and Koutouros, I., 2016, "Constitutive Model for Reinforcing Steel under Cyclic Loading," *Journal of Structural Engineering*, ASCE, V. 142, No. 12, 14 pp. doi: 10.1061/(ASCE)ST.1943-41X.001593
- Korentz, J., 2010, "The Effect of Yield Strength on Inelastic Buckling of Reinforcing Bars," *Mechanics and Mechanical Engineering*, V. 14, No. 2, pp. 247-255.
- Korentz, J., and Marcinowski, J., 2016, "Effect of Mechanical Parameters of Steel on Inelastic Buckling of Reinforcing Bars," *International Journal of Structural Stability and Dynamics*, V. 16, No. 7, 12 pp. doi: 10.1142/S0219455415500285
- Kunnath, S. K.; Heo, Y.; and Mohle, J. F., 2009, "Nonlinear Uniaxial Material Model for Reinforcing Steel Bars," *Journal of Structural Engineering*, ASCE, V. 135, No. 4, pp. 335-343. doi: 10.1061/(ASCE)0733-9445(2009)135:4(335)
- Lopes, A. V.; Lopes, S. M. R.; and do Carmo, R. N. F., 2012, "Effects of the Compressive Reinforcement Buckling on the Ductility of RC Beams in Bending," *Engineering Structures*, V. 37, pp. 14-23. doi: 10.1016/j.engstruct.2011.12.038
- Loya, A. S.; Lourenço, D. D. S.; Guner, S.; and Vecchio, F. J., 2016, "User's Manual of Janus for VecTor5," Online Publication, 28 pp., http://www.utoledo.edu/engineering/faculty/serhan-guner/docs/M2_VT5Janus-Manual_V2.0.pdf. (last accessed Jan. 7, 2019)
- Lynn, A.; Moehle, J. P.; Mahin, S. A.; and Holmes, W. T., 1996, "Seismic Evaluation of Existing Reinforced Concrete Building Columns," *Earthquake Spectra*, V. 12, No. 4, pp. 715-739. doi: 10.1193/1.1585907
- Maekawa, K.; Okamura, H.; and Pimanmas, A., 2003, *Nonlinear Mechanics of Reinforced Concrete*, Spon Press, London, UK, 768 pp.
- Mander, J. B.; Panthaki, F. D.; and Kasalanati, A., 1994, "Low-Cycle Fatigue Behavior of Reinforcing Steel," *Journal of Materials in Civil Engineering*, ASCE, V. 6, No. 4, pp. 453-468. doi: 10.1061/(ASCE)0899-1561(1994)6:4(453)
- Mander, J. B.; Priestley, M. J. N.; and Park, R., 1984, "Seismic Design of Bridge Piers," *Research Report 84-2*, Department of Civil Engineering, University of Canterbury, Christchurch, New Zealand.
- Mander, J. B.; Priestley, M. J. N.; and Park, R., 1988, "Theoretical Stress-Strain Model for Confined Concrete," *Journal of Structural Engineering*, ASCE, V. 114, No. 8, pp. 1804-1826. doi: 10.1061/(ASCE)0733-9445(1988)114:8(1804)
- Massone, L. M., and López, E. E., 2014, "Modeling of Reinforcement Global Buckling in RC elements," *Engineering Structures*, V. 59, pp. 484-494. doi: 10.1016/j.engstruct.2013.11.015
- Massone, L. M., and Moroder, D., 2009, "Buckling Modeling of Reinforcing Bars with Imperfections," *Engineering Structures*, V. 31, No. 3, pp. 758-767. doi: 10.1016/j.engstruct.2008.11.019
- Mau, S. T., and El-Mabsout, M., 1989, "Inelastic Buckling of Reinforcing Bars," *Journal of Engineering Mechanics*, ASCE, V. 115, No. 1, pp. 1-17. doi: 10.1061/(ASCE)0733-9399(1989)115:1(1)
- Monti, G., and Nuti, C., 1992, "Nonlinear Cyclic Behavior of Reinforcing Bars Including Buckling," *Journal of Structural Engineering*, ASCE, V. 118, No. 12, pp. 3268-3284. doi: 10.1061/(ASCE)0733-9445(1992)118:12(3268)
- Nojavan, A.; Schultz, A. E.; Chao, S.; and Haselton, C. B., 2017, "Influence of Cross-Sectional Size on Seismic Performance of Reinforced Concrete Columns," *ACI Structural Journal*, V. 114, No. 2, Mar.-Apr., pp. 311-321. doi: 10.14359/51689247
- Pantazopoulou, S. J., 1998, "Detailing for Reinforcement Stability in RC Members," *Journal of Structural Engineering*, ASCE, V. 124, No. 6, pp. 623-632. doi: 10.1061/(ASCE)0733-9445(1998)124:6(623)
- Prota, A.; de Cicco, F. D.; and Cosenza, E., 2009, "Cyclic Behavior of Smooth Steel Reinforcing Bars: Experimental Analysis and Modeling Issues," *Journal of Earthquake Engineering*, V. 13, No. 4, pp. 500-519. doi: 10.1080/13632460902837686
- Rodriguez, M. E.; Botero, J. C.; and Villa, J., 1999, "Cyclic Stress-Strain Behavior of Reinforcing Steel Including Effect of Buckling," *Journal of Structural Engineering*, ASCE, V. 125, No. 6, pp. 605-612. doi: 10.1061/(ASCE)0733-9445(1999)125:6(605)
- Saatcioglu, M., and Ozcebe, G., 1989, "Response of Reinforced Concrete Columns to Simulated Seismic Loading," *ACI Structural Journal*, V. 86, No. 1, Jan.-Feb., pp. 3-12.
- Sadeghian, V., 2012, "FormWorks-Plus: Improved Pre-Processor for VecTor Analysis Software," MASC Thesis, University of Toronto, Toronto, ON, Canada.

Sezen, H., and Moehle, J. P., 2002, "Seismic Behavior of Shear-Critical Reinforced Concrete Building Columns," Seventh U.S. National Conference on Earthquake Engineering, Earthquake Engineering Research Institute, Boston, MA.

Shanley, F. R., 1947, "Inelastic Column Theory," *Journal of the Aeronautical Sciences*, V. 14, No. 5, pp. 261-268. doi: 10.2514/8.1346

Shanley, F. R., 1950, "Applied Column Theory," *American Society of Civil Engineers*, Paper No. 2410, ASCE, Reprinted from Transactions, V. 115, pp. 698-727.

Soesianawati, M. T.; Park, R.; and Priestley, M. J. N., 1986, "Limited Ductility Design of Reinforced Concrete Columns," *Report 86-10*, Department of Civil Engineering, University of Canterbury, Christchurch, New Zealand, 208 pp.

Su, J.; Wang, J.; Bai, Z.; Wang, W.; and Zhao, D., 2015, "Influence of Reinforcement Buckling on the Seismic Performance of Reinforced Concrete Columns," *Engineering Structures*, V. 103, pp. 174-188. doi: 10.1016/j.engstruct.2015.09.007

Tanaka, H., and Park, R., 1990, "Effect of Lateral Confining Reinforcement on the Ductile Behavior of Reinforced Concrete Columns," *Report 90-2*, Department of Civil Engineering, University of Canterbury, Christchurch, New Zealand, 458 pp.

Tsuchiya, S.; Ogasawara, M.; Tsuno, K.; Ichikawa, H.; and Maekawa, K., 1999, "Multiaxial Flexural Behavior and Nonlinear Analysis of RC Columns Subjected to Eccentric Axial Forces," *Journal of Materials Concrete Structures and Pavements*, V. 634, No. 45, pp. 131-144.

Urmson, C. R., and Mander, J. B., 2012, "Local Buckling Analysis of Longitudinal Reinforcing Bars," *Journal of Structural Engineering*, ASCE, V. 138, No. 1, pp. 62-71. doi: 10.1061/(ASCE)ST.1943-541X.0000414

Vecchio, F. J., 2000, "Disturbed Stress Field Model for Reinforced Concrete: Formulation," *Journal of Structural Engineering*, ASCE, V. 126, No. 9, pp. 1070-1077. doi: 10.1061/(ASCE)0733-9445(2000)126:9(1070)

VecTor5, 2018, "Computer Program for the Nonlinear Static and Dynamic Analysis of Concrete Frames," www.utoledo.edu/engineering/faculty/serhan-guner/Software.html. (last accessed Jan. 7, 2019)

Xiao, Y., and Martirosyan, A., 1998, "Seismic Performance of High-Strength Concrete Columns," *Journal of Structural Engineering*, ASCE, V. 124, No. 3, pp. 241-251. doi: 10.1061/(ASCE)0733-9445(1998)124:3(241)

Yang, H.; Wu, Y.; Mo, P.; and Chen, J., 2016, "Improved Nonlinear Cyclic Stress-Strain Model for Reinforcing Bars Including Buckling Effect and Experimental Verification," *International Journal of Structural Stability and Dynamics*, V. 16, No. 1, 16 pp.

Zong, Z.; Kunnath, S.; and Monti, G., 2013, "Simulation of Reinforcing Bar Buckling in Circular Reinforced Concrete Columns," *ACI Structural Journal*, V. 110, No. 4, July-Aug., pp. 607-616.

Zong, Z.; Kunnath, S.; and Monti, G., 2014, "Material Model Incorporating Buckling of Reinforcing Bars in RC Columns," *Journal of Structural Engineering*, ASCE, V. 140, No. 1, pp. 1-10. doi: 10.1061/(ASCE)ST.1943-541X.0000808

Appendix to ACI Paper

Paper Title: A Constitutive Model for the Inelastic Buckling Behavior of Reinforcing Bars

Authors: Yildir Akkaya, Serhan Guner, Frank J. Vecchio

Summary: This appendix provides: in **Table A-1**, the data of 45 experimental reinforcing bars; in **Table A-2**, the data of 41 analytical reinforcing bars; in **Table A-3**, the default material model properties for the global analysis procedure; in **Tables A-4 to A-6**, the data of 16 axially and laterally-loaded columns; in **Tables A-7 to A-9**, the data from 4 beams; in **Fig. A-1**, verification of the DM and RDM models with the experimental and analytical data of reinforcing bars; in **Fig. A-2**, the analytical data from 29 reinforcing bar specimens produced by three different research groups, used to verify the DM and RDM models; in **Fig. A-3**, the data produced from the RDM and DM models for reinforcing bars having various geometric and material properties; in **Fig. A-4(a)**, the details of axially-loaded columns; in **Fig. A-4(b)** and **A-5**, the data used for verification with 10 axially and laterally-loaded columns; in **Fig. A-6**, the details and verification of the beams; and references cited in this appendix.

Table A-1 – Reinforcing bar specimens in the experiment dataset

Geometric and material properties											
Specimens		Diameter (D)		L/D	f_y		ϵ_y	$\epsilon_{sh} / \epsilon_y$	ϵ_u / ϵ_y	f_u / f_y	
*	**	(mm)	(in)	-	(MPa)	(ksi)	($\times 10^{-3}$)	-	-	-	
A	3	16	0.63	6,10,15	295.0	42.8	1.48	16.9	129.0	1.47	
B1	3	16,20,24	0.63,0.79,0.95	5,8,11	480.0	69.6	2.40	1.0	16.0	1.40	
B2	1	16	0.63	11	430.0	62.4	2.40	2.9	29.2	1.29	
B3	1	16	0.63	11	430.0	62.4	2.70	3.7	25.9	1.47	
C	6	20	0.79	5-10	520	75.4	2.60	3.8	57.7	1.34	
D1	8	25.4	1.00	5-12	437.0	63.4	2.20	4.2	66.8	1.67	
D2	8	32.3	1.27	5-12	444.0	64.4	2.20	4.1	71.8	1.44	
E1	1	12	0.47	15	327.0	47.4	1.60	2.0	144.4	1.34	
E2	4	12	0.47	5,10,15,20	338.4	49.1	1.80	13.9	111.1	1.39	
E3	2	14	0.55	5,8	351.5	51.0	2.10	1.1	95.2	1.26	
E4	4	14	0.55	5,10,15,20	534.0	77.4	2.80	2.2	71.4	1.58	
E5	4	14	0.55	5,10,15,20	540.0	78.3	3.00	8.2	38.3	1.18	

* A=Mander (1984), B=Monti and Nuti (1992), C=Bayrak and Sheikh (2001),
 * D=Bae et al. (2005), E=Prota et al. (2009) ** Number of specimens tested experimentally

Table A-2 – Reinforcing bar specimens in the analytical dataset

Geometric and material properties										
Specimens		Diameter (D)		L/D	f _y		ε _y	ε _{sh} / ε _y	ε _u / ε _y	f _u /f _y
*	**	(mm)	(in)	-	(MPa)	(ksi)	(x10 ⁻³)	-	***	-
F1	7	25.4	1.00	6-14	476.0	69.0	2.38	4.7	25.2	1.74
F2	8	25.4	1.00	6-15	410	60.0	2.05	50.0	50.0	1.00
G1	4	16	0.63	6.3-18.8	400.0	58.0	2.00	5.0	60.0	1.50
G2	3	25	0.99	6-12	400.0	58.0	2.00	5.0	60.0	1.50
H1	4	16	0.63	10	200-800	29-116	1.0-4.0	24.0	24.0	1.00
H2	4	16	0.63	10	200-800	29-116	1.0-4.0	5.0	20.0	1.25
H3	4	16	0.63	10	200-800	29-116	1.0-4.0	10.0	50.0	1.50
H4	4	16	0.63	10	200-800	29-116	1.0-4.0	15.0	135.0	1.75
H5	3	16	0.63	5	800	116.0	4.0	5-15	20-135	1.25-1.75

* F=Mau and El-Mabsout (1989), G=Gil-Martin et al. (2006), H=Korentz (2010)

** Number of specimens tested analytically, ***ε_u was chosen to obtain similar tension curve with P=4

Table A-3 – Default material models used (Wong et al. 2013).

Material behaviour	Default model	Material behaviour	Default model
Compression base curve	Popovics	Concrete hysteresis	Nonlinear w/ plastic offsets
Compression post-peak	Modified Park-Kent	Slip distortion	Walraven
Compression softening	Vecchio 1992-A	Strain rate effects	fib Model Code - Malvar
Tension stiffening	Modified Bentz 2003	Rebar hysteresis	Seckin w/ Bauschinger
Tension softening	Linear	Rebar dowel action	Tassios (Crack slip)
Confinement strength	Kupfer / Richart	Rebar buckling	DM or RDM (as noted)
Cracking criterion	Mohr-Coulomb (Stress)	Geometric nonlinearity	Considered
Crack width check	Agg/5 Max crack width	Previous loading history	Considered

Table A-4 – Axially- and laterally-loaded column specimens

*	RC column Specimen name	Analy. model	Sect. type	**ALR	L _c		h=b		f _c '	
					mm	in.	mm	in.	MPa	ksi
A	S2, S3	DE	I, II	0.2	1600	63.0	400	15.8	25.6	3.7
B	AS-2HT, AS-3HT	DE	IV	0.36, 0.50	1473	58.0	305	12.0	71.7	10.4
C	U3	CFB	III	0.14	1000	39.4	350	13.8	34.8	5.1
C	U4	CFB	III	0.15	1000	39.4	350	13.8	32.0	4.6
D	SNo1	DE	VI	0.10	1600	63.0	400	15.8	46.5	6.7
D	SNo2	DE	VI	0.30	1600	63.0	400	15.8	44.0	6.4
E	HC48L16T601P	DC	I	0.1	1016	40.0	254	10.0	86.0	12.5
E	HC48L16T602P	DC	I	0.2	1016	40.0	254	10.0	86.0	12.5
F	SMNo-1, SMNo-4	DC	IV	0.15, 0.14	2946	58.0	457	18.0	21.4	3.1
G	2CLH18	DC	V	0.07	2946	58.0	457	18.0	33.1	4.8
G	2CMH18	DC	V	0.28	2946	58.0	457	18.0	25.5	3.7
G	3CLH18, 3CMH18	DC	V	0.09, 0.26	2946	58.0	457	18.0	27.3	4.0

* A: Tanaka and Park (1990), B: Bayrak and Sheikh (1997), C: Saatcioglu and Ozcebe (1989),
D: Soesianawati et al. (1986), E: Xiao and Martirosyan (1998), F: Sezen and Moehle (2002),
G: Lynn et al. (1996) ** ALR= Axial load ratio

Table A-5 – Longitudinal reinforcing bars for columns

RC column Specimen no	Longitudinal reinforcement								
	Ratio	Diameter (d _b)		f _y		ε _y	*ε _{sh}	*ε _u	*f _u /f _y
	(%)	(mm)	(in)	(MPa)	(ksi)	(x10 ⁻³)			-
S2, S3	1.57	20	0.79	474.0	68.7	2.37	10	160	1.52
AS-2HT, AS-3HT	2.58	19.5	0.77	454.0	65.8	2.27	7	130	1.54
U3	3.21	25	0.99	430.0	62.4	2.15	10	180	1.35
U4	3.21	25	0.99	438.0	63.5	2.19	10	180	1.35
SNo1, SNo2	1.51	16	0.63	446.0	64.7	2.23	10	160	1.57
HC48L16T601P	2.46	15.9	0.63	510.0	74.0	2.55	10	80	1.30
HC48L16T602P	2.46	15.9	0.63	510.0	74.0	2.55	10	50	1.30
SMNo-1, SMNo-4	2.47	28.7	1.13	434.4	62.9	2.17	5	40	1.49
2CLH18, 2CMH18	1.94	25.4	1.0	331.0	48.0	1.66	10	80	1.50
3CLH18, 3CMH18	3.03	31.8	1.25	331.0	48.0	1.66	10	40-50	1.50

* Assumed values in the analysis

Table A-6 – Transverse reinforcing bars for columns

RC column	Transverse reinforcement						
Specimen no	s		Diameter (d_t)		f_y		$*f_u/f_y$
	(mm)	(in.)	(mm)	(in.)	(MPa)	(ksi)	-
S2, S3	80	3.2	12	0.47	333.0	48.3	1.44
AS-2HT, AS-3HT	90	3.5	11.3	0.45	542	78.6	1.26
U3, U4	75, 50	3.0, 2.0	10	0.39	470.0	68.1	1.45
SNo1	85	3.3	7	0.28	364.0	52.8	1.43
SNo2	78	3.1	8	0.32	360	52.2	1.37
HC48L16T601P-02P	51	2.0	6.4	0.25	449	65.1	1.30
SMNo1, SMNo4	305	12.0	9.5	0.37	476	69.0	1.52
2CLH18, 2CMH18	457	18.0	9.5	0.37	400	58	1.4
3CLH18, 3CMH18	457	18.0	9.5	0.37	400	58	1.4

* Assumed values in the analysis (experimental values are not reported).

$E_s=200$ GPa (2.9×10^4 ksi), $\epsilon_{sh}=0.01$

Table A-7 – Longitudinal reinforcing bars in tension and concrete strength of S-beams

RC beam	Longitudinal reinforcing bars in tension							Concrete strength	
Specimen	ρ	ρ_b	Diameter (d_b)		f_y		f_u/f_y	f_c'	
*No	(%)	(%)	(mm)	(in)	(MPa)	(ksi)	-	(MPa)	(ksi)
S1B2	2.50	1.38	20	0.79	619	89.8	1.17	24.0	3.5
S1B3	2.46	1.73	16	0.63	531	77.0	1.22	24.0	3.5
S3B2, S3B3	2.50	1.74	20	0.79	619	89.8	1.17	31.0	4.5

*All specimens were tested and reported by Lopes et al. (2012).

Table A-8 – Longitudinal reinforcing bars in compression of S-beams

RC beam	Longitudinal reinforcing bars in compression						Buckling parameters	
Specimen	ρ'	Diameter (D)		f_y		f_u/f_y	*L/D	r_b
No	(%)	(mm)	(in)	(MPa)	(ksi)	-	-	-
S1B2	0.11	6	0.24	587	85.1	1.13	9	22
S1B3	0.80	16	0.63	531	77.0	1.21	12	28
S3B2, S3B3	0.11	6	0.24	571	82.8	1.07	15, 8	36, 19

*Calculated value from the proposed method by Dhakal and Maekawa (2002c).

Table A-9 – Transverse reinforcing bars of S-beams

RC beam	*Transverse reinforcing Bars					Reinforcement ratios	
Specimen	Tie spacing (s)		f_y		f_u/f_y	ρ_t	** ρ_z
No	(mm)	(in)	(MPa)	(ksi)	-	(%)	(%)
S1B2	50	2.0	587	85.1	1.13	0.566	0.146
S1B3	45	1.8	587	85.1	1.13	0.629	0.210
S3B2, S3B3	90, 45	3.6, 1.8	571	82.8	1.07	0.314, 0.629	0.063, 0.170

*Diameter of transverse reinforcing bars is 6 mm (0.24 in.) for all specimens

** Values of ρ_z were calculated from the proposed method by Mander et al. (1988)

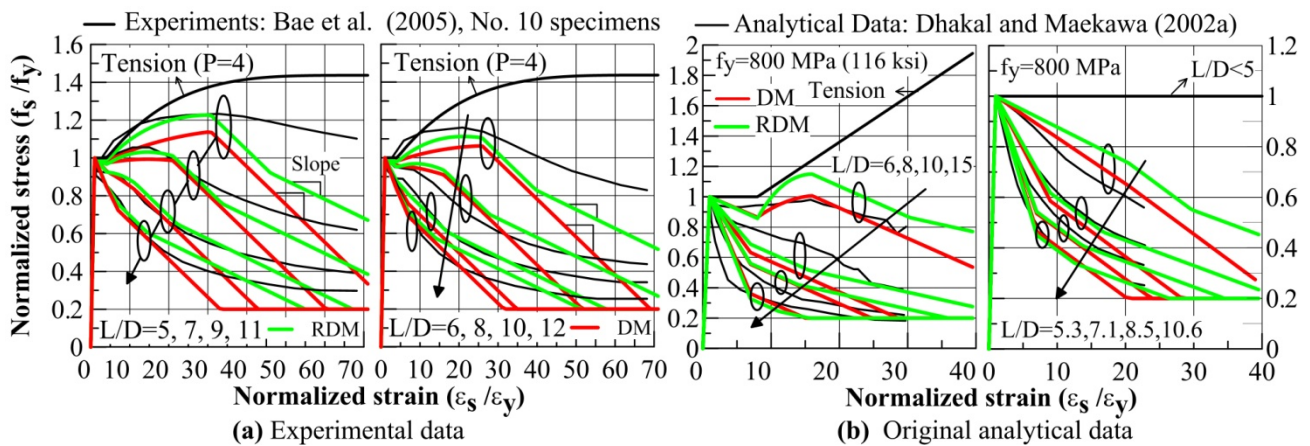


Fig. A-1 – Verification results with the experimental and analytical data of reinforcing bars

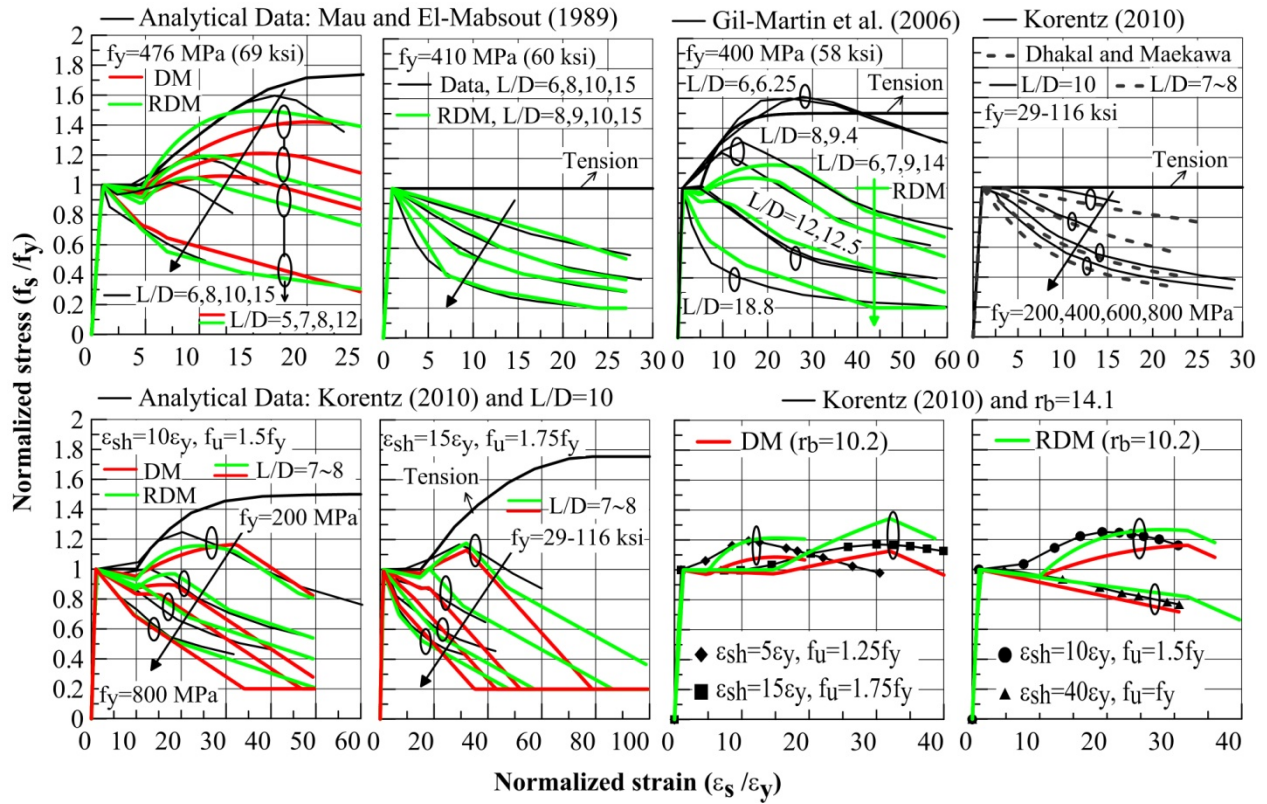


Fig. A-2 – Verification with analytical data produced by various researchers

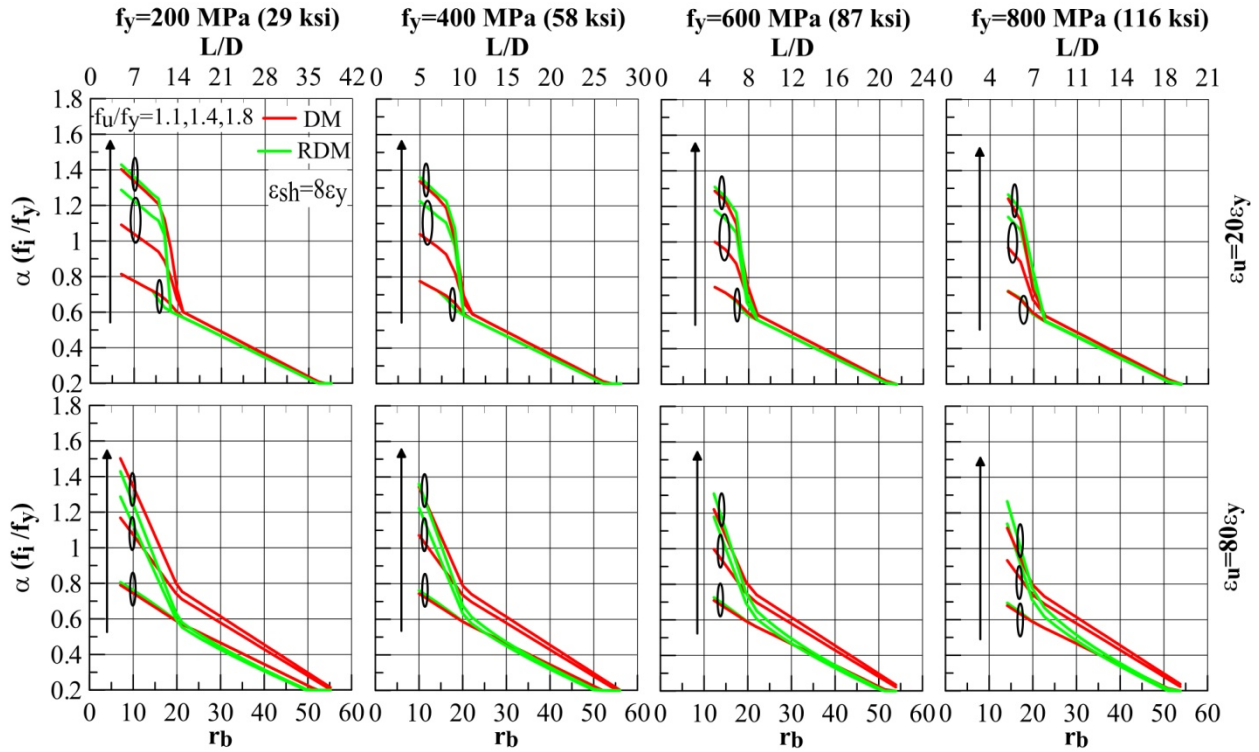


Fig. A-3 – Comparison of the normalized intermediate stress (f_i/f_y) values for various geometric and material properties of the reinforcing bars.

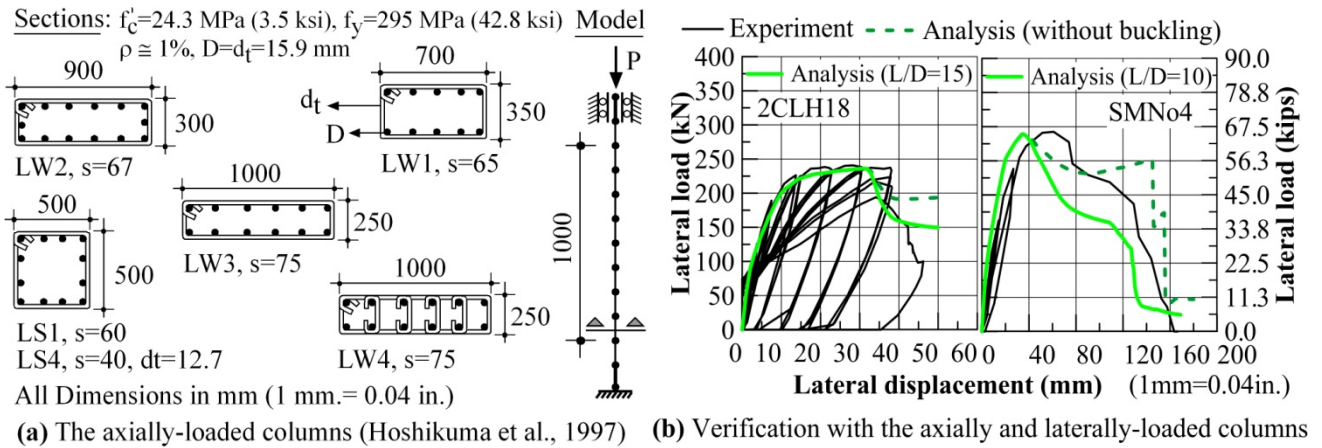


Fig. A-4 – Geometry details and verification results with column specimens

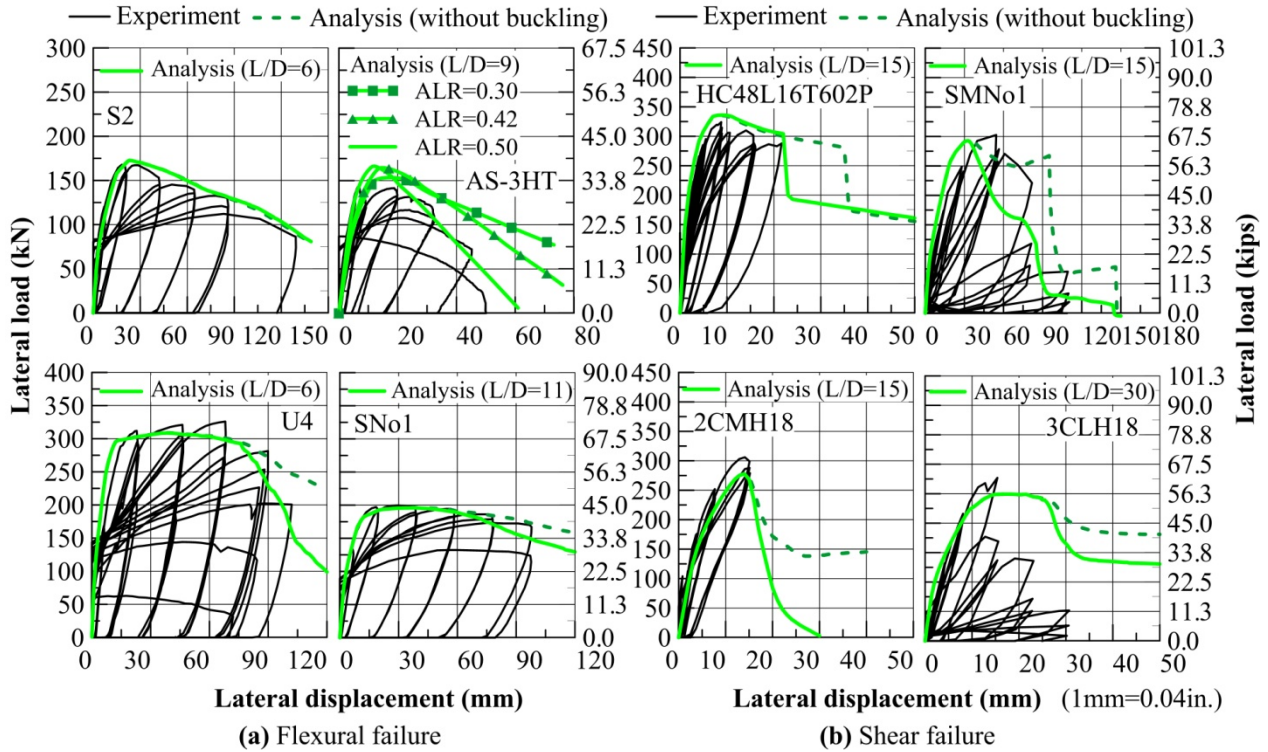


Fig. A-5 – Verification results with the axially- and laterally-loaded columns

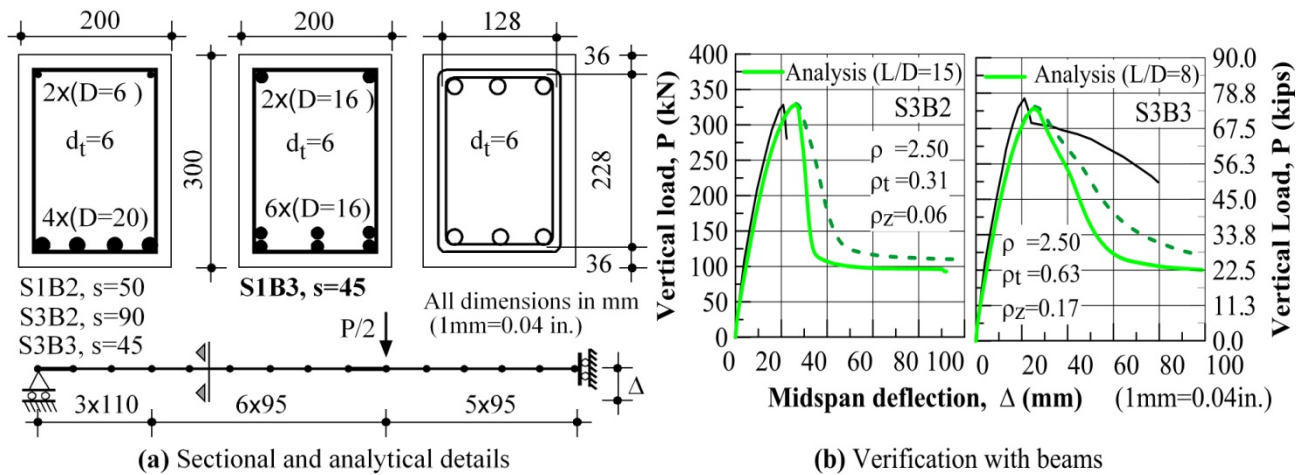


Fig. A-6 – Beams Tested by Lopes et al. (2012)

APPENDIX REFERENCES

- Berry, M.P., and Eberhard, M.O., 2005, "Practical Performance Model for Bar Buckling," *Journal of Structural Engineering*, ASCE, V.131, No. 7, pp. 1060-1070.
- Bresler, B., and Gilbert, P.H., 1961, "Tie Requirements for Reinforced Concrete Columns," *ACI Journal, Proceedings*, V. 58, No. 5, pp. 555-570.
- Cosenza, E., and Prota, A., 2006, "Experimental Behavior and Numerical Modeling of Smooth Steel Bars under Compression," *Journal of Earthquake Engineering*, V. 10, No. 19, pp. 313-329.
- Dodd, L.L., and Restrepo-Posada, J.I., 1995, "Model for Predicting Cyclic Behavior of Reinforcing Steel," *Journal of Structural Engineering*, ASCE, V. 121, pp. 433-445.
- Gomes, A., and Appleton, J., 1997, "Nonlinear Cyclic Stress-Strain Relationship of Reinforcing Bars Including Buckling," *Engineering Structures*, V. 19, pp. 822-826.
- Kim, S.H., and Koutromanos, I., 2016, "Constitutive Model for Reinforcing Steel under Cyclic Loading," *Journal of Structural Engineering*, ASCE, V. 142, No. 12, 04016133, pp. 14.
- Korentz, J., and Marcinowski J., 2016, "Effect of Mechanical Parameters of Steel on Inelastic Buckling of Reinforcing Bars," *International Journal of Structural Stability and Dynamics*, V. 16, No. 7, 1550028, 12 pp.
- Mander, J.B.; Panthaki, F.D.; and Kasalanati, A., 1994, "Low-Cycle Fatigue Behavior of Reinforcing Steel," *Journal of Materials in Civil Engineering*, V. 6, No.4, pp. 453-468.
- Massone, L.M., and López E.E., 2014, "Modeling of Reinforcement Global Buckling in RC elements," *Engineering Structures*, V. 59, pp. 484-494.
- Massone, L.M., and Moroder, D., 2009, "Buckling Modeling of Reinforcing Bars with Imperfections," *Engineering Structures*, V. 31, pp. 758-767.
- Nojavan, A.; Schultz, A.E.; Chao, S.; and Haselton C.B., 2017, "Influence of Cross-Sectional Size on Seismic Performance of Reinforced Concrete Columns," *ACI Structural Journal*, V. 114, No. 2, pp. 311-321.
- Pantazopoulou, S.J., 1998, "Detailing for Reinforcement Stability in RC Members," *Journal of Structural Engineering*, V. 124, N. 6, pp. 623-632.
- Rodriguez M.E.; Botero J.C.; and Villa J., 1999, "Cyclic Stress-Strain Behavior of Reinforcing Steel Including Effect of Buckling," *Journal of Structural Engineering*, ASCE, V. 125, No. 6, pp. 605-612.
- Shanley, F.R., 1947, "Inelastic Column Theory," *Journal of Aeronautical Sciences*, V. 14, No. 5, pp. 261-264.
- Shanley, F.R., 1950, "Applied Column Theory," *American Society of Civil Engineers*, ASCE, Paper No. 2410, Reprinted from Transactions, V. 115, pp. 698-727.
- Su, J.; Wang, J.; Bai, Z.; Wang, W.; and Zhao, D., 2015, "Influence of Reinforcement Buckling on the Seismic Performance of Reinforced Concrete Columns," *Engineering Structures*, V. 103, pp. 174-188.
- Wong P.S.; Vecchio F.J.; and Trommels H., 2013, "VecTor2 and FormWorks User's Manual," Technical Report, Department of Civil Engineering, University of Toronto, Canada, 318 pp., http://vectoranalysisgroup.com/user_manuals/manual1.pdf (last access: March 10, 2018)

Yang, H.; Wu, Y.; Mo, P.; and Chen, J., 2016, "Improved Nonlinear Cyclic Stress-Strain Model for Reinforcing Bars Including Buckling Effect and Experimental Verification," *International Journal of Structural Stability and Dynamics*, V. 16, No. 1, 1640005, 16 pp.

Zong, Z.; Kunnath, S.; and Monti G., 2013, "Simulation of Reinforcing Bar Buckling in Circular Reinforced Concrete Columns," *ACI Structural Journal*, V. 110, No. 4, pp. 607-616.

Zong, Z.; Kunnath, S.; and Monti G., 2014, "Material Model Incorporating Buckling of Reinforcing Bars in RC Columns," *Journal of Structural Engineering*, ASCE, V. 140, pp. 1-10.